

Faculty of Informatics

Faculty of Informatics - Papers

University of Wollongong

Year 2005

Generalized Analysis Model for Fringe
Pattern Profilometry

Y. Hu* J. Xi† Z. Yang‡
E. Li** J. F. Chicharo††

*University of Wollongong, yingsong@uow.edu.au

†University of Wollongong, jiangtao@uow.edu.au

‡Huazhong University of Science & Technology, China

**University of Wollongong, enbang@uow.edu.au

††University of Wollongong, chicharo@uow.edu.au

This paper originally appeared as: Hu, Y, Xi, J, Yang, Z et al, Generalized Analysis Model for Fringe Pattern Profilometry, Proceedings of the IEEE Instrumentation and Measurement Technology Conference, 16-19 May 2005, vol 3, 1951-1955. Copyright IEEE 2005.

This paper is posted at Research Online.

<http://ro.uow.edu.au/infopapers/247>

Generalized Analysis Model for Fringe Pattern Profilometry

Yingsong Hu^{1,2}, Jiangtao Xi², Zongkai Yang¹, Enbang Li², Joe Chicharo²

¹ Department of Electronic and Information Engineering,
Huazhong University of Science and Technology,
Wuhan City, China.

² School of Electrical Computer and Telecommunications Engineering,
University of Wollongong,
Wollongong, NSW 2522, Australia.
E-mail: yingsong@uow.edu.au.

Abstract – In this paper, a generalized analysis model for fringe pattern profilometry is presented. The new analysis model is derived mathematically, which describes the essential relationships between projected and deformed fringe patterns. With generalized analysis model, the projected fringe patterns used for profilometry can be arbitrary rather than being limited to be sinusoidal as those for the conventional approaches. Meanwhile, based on the proposed generalized model, a new algorithm is presented to reconstruct three-dimensional surfaces. Computer simulation results show that compared with the conventional model for fringe pattern profilometry, the generalized model and the proposed algorithm can significantly improve the three-dimensional reconstruction accuracy, especially when the projected fringe pattern is distorted by some unknown factors.

Keywords – fringe pattern profilometry, fringe pattern analysis.

I. INTRODUCTION

Fringe pattern profilometry (FPP) is one of the most popular non-contact methods for measuring the three-dimensional object surfaces in recent years. With fringe pattern profilometry (FPP), a Ronchi grating or sinusoidal grating is used to project fringe patterns onto a three-dimensional diffuse surface which results in deformed fringe patterns. The images of the deformed fringe pattern and the original fringe pattern projected on a reference plane are captured by a CCD camera and are processed to reconstruct the profile of objects. In order to reconstruct the 3-D surface information from the fringe pattern images, a number of fringe pattern analysis methods have been developed, including Fourier Transform Profilometry (FTP)[1], [2], [3], [4], Phase Shifting Profilometry (PSP)[5], [6], [7], [8], Spatial Phase Detection (SPD)[9], Phase Locked Loop (PLL)[10] and other analysis methods[11], [12].

There are various methods to generate fringe patterns. In recent years, digital projectors have been widely used to obtain fringe patterns[13], [14], [15]. The advantage of utilizing digital projectors for fringe pattern profilometry (FPP) is its simplicity and controllability. However, it is very difficult to obtain a pure sinusoidal fringe pattern by digital projectors

due to the existence of geometrical distortion and colour distortion. Meanwhile we can note that for all the methods mentioned above, it has been assumed that fringe patterns used for profilometry are pure sinusoidal or can be filtered to be sinusoidal by using digital filters to pick up the fundamental frequency component while eliminating the higher harmonics. However, in most practical cases, the filter can not be ideal and the results are still not pure sinusoidal. Additionally, when the deformed fringe pattern has an overlapped spectra, bandpass filtering will be unusable if a precise measurement is required. Therefore, errors will arise if the surface measurement is based on pure sinusoidal assumption. This problem motivates us to look for a new method to reconstruct the 3-D profile based on non-sinusoidal fringe patterns.

In this paper, we present a generalized analysis model which describes a general relationship between the projected signal and the deformed signal in profilometry systems. The derived mathematical model does not require the fringe pattern pure sinusoidal or of some other particular structures. This also implies that theoretically, distorted sinusoidal fringe patterns are still useful for profilometry.

Based on the derived mathematical model, this paper also proposes a new algorithm, referred to as shift estimation (SE) method, to reconstruct 3-D surfaces using fringe pattern profilometry (FPP) technique. Compared with traditional methods, our algorithm has neither the requirement for the structure of projected fringe patterns, nor the prior knowledge of the characteristics of projection systems. The correctness of the proposed mathematical model and shift estimation (SE) method has been confirmed by simulation results, which are provided to demonstrate that compared with the conventional analysis methods, the measurement accuracy has been significantly improved by shift estimation (SE) method, especially when the expected sinusoidal fringe patterns are distorted by unknown factors.

This paper is organized as follows. In Section II, a generalized model for fringe pattern profilometry is mathematically derived and briefly compared with traditional analysis model.

In Section III, shift estimation (SE) method is presented to reconstruct the 3-D surface based on the generalized model proposed in Section II. In Section IV, we give our comparative simulation results to confirm the correctness of the generalized analysis model and demonstrate the improvement of using shift estimation (SE) method. Section V concludes this paper.

II. GENERALIZED ANALYSIS MODEL

A schematic diagram of a typical fringe pattern profilometry (FPP) system is shown in Fig.1. For the sake of simplicity

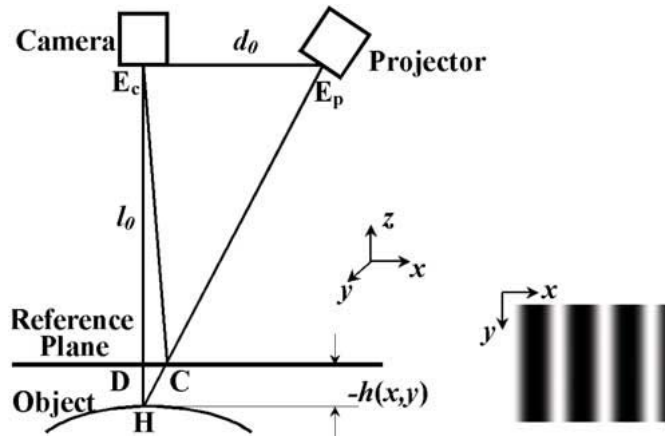


Fig. 1. Schematic diagram of fringe pattern profilometry (FPP) system

we assume that the distance between the camera and the reference plane is long enough so that the reflected light beams captured by CCD camera from the reference plane and object are parallel. Meanwhile, because of the long distance, those parallel light beams reflected to the camera can be regarded as being vertical to the reference plane. The fringe pattern projected onto the reference plane is denoted by $s(x, y)$, which is the intensity of the signal at the location of (x, y) where x, y axes and a typical fringe pattern are depicted in Fig.1. Similarly the intensity of the deformed fringe pattern is denoted by $d(x, y)$.

As shown in Fig.1, the projected fringe pattern on the reference plane is designed to exhibit a constant intensity along the y direction. Hence we can simply consider the signal intensity along the x direction for any given y coordinate, and the results can be extended to other values of y . i.e. we only consider cross sections of the object surface for given y coordinates. Therefore, instead of $s(x, y)$ and $d(x, y)$, we simply use $s(x)$ and $d(x)$ to denote the projected signal on the reference plane and the deformed signal respectively. Similarly the height distribution function $h(x, y)$ of the object surface can also be represented as $h(x)$, a function with only one independent variable x , when we are considering the sections of object surfaces.

In order to establish the relationship between $s(x)$ and $d(x)$, we consider a beam of light corresponding to a pixel of the

fringe pattern, denoted as E_pCH in Fig.1. It is seen that the light beam is projected at point C and reflected back to the camera if the reference plane exists. When the reference plane is removed, the same beam will be projected onto point H on the surface of the object, which is reflected to the camera via point D. This implies that the x coordinate of point H in the image of object surface equals to the x coordinate of point D in the image of reference plane, because point D and H are on the same reflected beam from point H to the camera. Assuming that the object surface and the reference plane have the same reflective characteristics, $s(x)$ at location C should exhibit the same intensity as $d(x)$ does at location D because they originate from the same point of the fringe pattern created by the projector. Hence we have

$$d(x_d) = s(x_c) \quad (1)$$

We use u to denote the distance from C to D, that is

$$u = x_d - x_c \quad (2)$$

where x_c and x_d are the coordinate locations of point C and point D, respectively. From Eqs.(1) and (2), we have

$$d(x_d) = s(x_d - u) \quad (3)$$

Obviously, u varies with the height of point H on the object surface.

Meanwhile, because triangles E_pHE_c and CHD are similar, we have

$$\frac{x_c - x_d}{-h(x_h)} = \frac{d_0}{l_0 - h(x_h)} \quad (4)$$

where x_h is the x coordinate of point H, l_0 is the distance between the camera and the reference plane and d_0 is the distance between the camera and the projector.

As mentioned above, point H has the same x coordinate as point D does in captured images, which implies $x_h = x_d$. So Eq.(4) can be rewritten as

$$\frac{x_c - x_d}{-h(x_d)} = \frac{d_0}{l_0 - h(x_d)} \quad (5)$$

As defined in Eq.(2), Eq.(5) can be expressed as

$$\frac{-u}{-h(x_d)} = \frac{d_0}{l_0 - h(x_d)} \quad (6)$$

As the height distribution $h(x)$ is a function of x_d , u should be also a function of x_d . Then we have

$$u(x_d) = \frac{d_0 h(x_d)}{l_0 - h(x_d)} \quad (7)$$

An equivalent representation is

$$h(x_d) = \frac{l_0 u(x_d)}{d_0 + u(x_d)} \quad (8)$$

Therefore, Eq.(3) can be expressed as

$$d(x_d) = s(x_d - u(x_d)) \quad (9)$$

where $u(x_d)$ is given by Eq.(7).

To simplify Eq.(9) and consider the model only mathematically, we let $x_d = x$, then we can derive a general mathematical model from Eqs.(8) and (9).

$$d(x) = s(x - u(x)) \quad (10)$$

$$h(x) = \frac{l_0 u(x)}{d_0 + u(x)} \quad (11)$$

Eq.(10) and Eq.(11) reveal that the deformed signal $d(x)$ is a shifted version of $s(x)$, and the shift function $u(x)$ varies with the height of the object. This implies that the shift signal $u(x)$ contains all the 3-D information of the object surface. By using Eqs.(10) and (11), as long as we can obtain the function $u(x)$, the surface reconstruction can be achieved.

Eq.(10) expresses the general relationship between the deformed signal and the projected signal. Note that the projected signal $s(x)$ can be of any form and hence it is not necessarily required to be sinusoidal. Therefore, compared with traditional model, Eq.(10) and Eq.(11) can be regarded as a generalized analysis model for fringe pattern profilometry, and the conventional analysis model is only a special case of the generalized model proposed above. They would have a consistent form when cosinusoidal fringe patterns are projected onto object surfaces. Actually by letting $s(x)$ be cosinusoidal signal, we can simply derive the traditional analysis model from our proposed generalized model. If we use sinusoidal or cosinusoidal fringe patterns, the projected signal can be expressed as:

$$s(x) = A + B \cos(2\pi f_0 x) \quad (12)$$

where A is the background illumination which can be regarded as a constant and B is the amplitude of intensity of cosinusoidal fringe patterns. By substituting Eq.(12) into Eq.(11), the deformed signal is

$$\begin{aligned} d(x) &= s(x - u(x)) \\ &= A + B \cos(2\pi f_0(x - u(x))) \\ &= A + B \cos(2\pi f_0 x - 2\pi f_0 u(x)) \\ &= A + B \cos(2\pi f_0 x + \phi(x)) \end{aligned} \quad (13)$$

where

$$\phi(x) = -2\pi f_0 u(x) \quad (14)$$

As expected, for the case where a cosinusoidal fringe pattern is used, the deformed signal $d(x)$ is a phase-modulated signal. Hence, all of the conventional analysis methods attempt to demodulate the deformed signals and retrieve the phase map $\phi(x)$ firstly. Then, by using the relationship between the phase shift function, $\phi(x)$, and the height distribution $h(x)$, the shapes of objects can be reconstructed. Actually, when a

sinusoidal fringe pattern is used, we can easily derive the relationship between $\phi(x)$ and $h(x)$ by our proposed generalized model. Note in Eq.(14), an equivalent form is:

$$u(x) = -\frac{\phi(x)}{2\pi f_0} \quad (15)$$

By substituting Eq.(15) into Eq.(11), we can derive a well-known equation:

$$h(x) = \frac{l_0 \phi(x)}{\phi(x) - 2\pi f_0 d_0} \quad (16)$$

An equivalent form of Eq.(16) is

$$\phi(x) = \frac{2\pi f_0 d_0 h(x)}{h(x) - l_0} \quad (17)$$

As classical formulas, Eq.(16) and Eq.(17) appear in most of the articles on fringe pattern profilometry (for example [2], [4], [16]).

As mentioned above, essentially, the conventional model is simply a particular case of our proposed model when the projected signal on the reference plane $s(x)$ is exactly sinusoidal. However, in practical cases, especially when we are using a digital projector to generate fringe patterns, it is very difficult to obtain a pure sinusoidal signal. Fortunately, our proposed generalized model does not require the projected signal sinusoidal. That implies although the projected signal has been distorted by some unknown factors, accurate profilometry is still practicable, as long as we can find out a method to retrieve the shift signal $u(x)$ from the captured signals $s(x)$ and $d(x)$. Based on our proposed generalized model, we present an shift estimation (SE) method to retrieve the shift function $u(x)$ in the next section.

III. SHIFT ESTIMATION METHOD

According to the generalized model presented in Section II, the value of shift function $u(x)$ determines the height distribution $h(x)$, so that the height distribution of the object surface can be obtained if we have $u(x)$. Hence, we should track the values of shift function $u(x)$ for each point x by using $s(x)$ and $d(x)$. For this purpose, we use square error defined below as an objective function with respect to $\hat{u}(x)$ that denotes the estimation of the value of $u(x)$ at point x :

$$e^2(\hat{u}(x)) = [d(x) - s(x - \hat{u}(x))]^2 \quad (18)$$

In order to minimize the error e^2 , we use gradient-based method to obtain $\hat{u}(x)$ in an iterative way:

$$\hat{u}_{m+1} = \hat{u}_m - \eta \frac{de^2}{d\hat{u}} \Big|_{\hat{u}=\hat{u}_m} \quad (19)$$

where η is the learning rate. The gradient can be derived as:

$$\begin{aligned}
\frac{de^2}{d\hat{u}}|_{\hat{u}=\hat{u}_m} &= 2e \frac{de}{d\hat{u}}|_{\hat{u}=\hat{u}_m} = -2e \frac{ds}{d\hat{u}}|_{\hat{u}=\hat{u}_m} \\
&= -2e \frac{s(x - (\hat{u}_m + 1)) - s(x - (\hat{u}_m - 1))}{(\hat{u}_m + 1) - (\hat{u}_m - 1)} \\
&= -e[s(x - \hat{u}_m - 1) - s(x - \hat{u}_m + 1)] \\
&= -[d(x) - s(x - \hat{u}_m)] \times \\
&\quad [s(x - \hat{u}_m - 1) - s(x - \hat{u}_m + 1)] \quad (20)
\end{aligned}$$

Substituting Eq.(20) into Eq.(19), we can have an iterative equation to calculate the estimation of the value of shift function $u(x)$ at each point x .

$$\begin{aligned}
\hat{u}_{m+1}(x) &= \hat{u}_m(x) + \eta[d(x) - s(x - \hat{u}_m(x))] \times \\
&\quad [s(x - \hat{u}_m(x) - 1) - s(x - \hat{u}_m(x) + 1)] \quad (21)
\end{aligned}$$

For each point x , the iteration continues until convergence. In other words, if $|\hat{u}_{m+1} - \hat{u}_m|$ is less than a given lower bound, we can obtain an estimation of the value of $u(x)$ at point x , $\hat{u}(x) = \hat{u}_m(x)$. Considering the continuity of the profiles, we can use the converged value $\hat{u}(x)$ as the initial value for the next point $x + 1$. i.e. let $\hat{u}_1(x + 1) = \hat{u}(x)$ and then continue doing the iteration for the next point $x + 1$, so that faster convergence can be achieved.

IV. SIMULATION RESULTS

Simulations have been performed to verify the correctness of the generalized model and the effectiveness of our proposed shift estimation (SE) method. In our simulation, we use a paraboloid object surface whose maximum height is 160mm and the projected fringe pattern is generated from a cosinusoidal signal distorted by a nonlinear function given by:

$$s(g(x)) = 0.00156g^2(x) + g(x) + C \quad (22)$$

where C is a constant which can be ignored as it does not effect on reconstruction results, and $g(x) = A \cos(2\pi f_0 x)$ where f_0 is the spatial frequency of the fringe pattern, which is assumed to be 0.01/mm in our simulation. i.e. the spatial period of the fringe pattern is assumed to be 100mm. Assuming 8-bits quantification is used for CCD camera, A , the amplitude of the cosinusoidal signal $g(x)$ is assumed to be 128. Meanwhile, we assume l_0 and d_0 in Fig.1 equal to 5 meters and 2 meters respectively. The spatial resolution of the captured image is assumed to be 1 pixel/mm.

Substituting $g(x) = A \cos(2\pi f_0 x)$ into Eq.(22) and discarding DC component, we have:

$$s(x) = 128 \cos(2\pi f_0 x) + 12.8 \cos(2\pi \cdot (2f_0)x) \quad (23)$$

Note for the projected fringe pattern given by Eq.(23), the second order harmonic only has -20db of power compared with

the fundamental component. Corresponding to Eq.(23), the deformed fringe pattern can be expressed as:[2], [4]

$$d(x) = 128 \cos(2\pi f_0 x + \phi(x)) + 12.8 \cos(2\pi \cdot (2f_0)x + 2\phi(x)) \quad (24)$$

where $\phi(x)$ is the phase shift caused by the object surface. It has been well-known that with conventional model, after demodulating $\phi(x)$, the surface height distribution can be calculated by the relationship between $\phi(x)$ and the height distribution $h(x)$, which is expressed as Eq.(16).

Using the fringe pattern given by Eq.(23) and Eq.(24), we can reconstruct the object surface by conventional PSP method and shift estimation (SE) method respectively. The comparative results are shown in Fig.2. In Fig.2(a), The solid line is

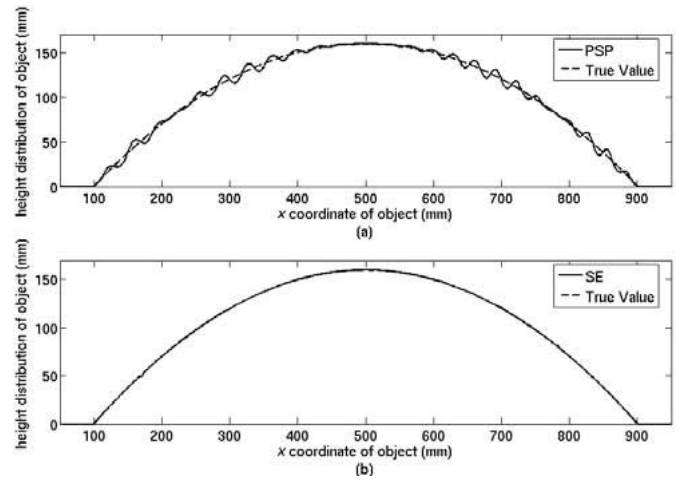


Fig. 2. Reconstruction results and error comparison

the measurement result by PSP method, while the dashed line refers to the object surface, which is the true value of the height distribution. This figure shows nonlinear distortion introduces noticeable errors when PSP method is used, even though the nonlinear distortion is so slight that coefficient of square item in Eq.(22) is only 0.00156 and the second order harmonic only has -20db of power compared with fundamental component. Moreover, the reconstructed surface by using PSP method is jagged and not smooth.

Comparatively, by our proposed model and shift estimation (SE) method, we can obtain a much better reconstruction result shown in Fig.2(b). Same to Fig.2(a), dashed line is the true value and solid line represents the reconstruction result by using our proposed generalized model and shift estimation (SE) method. It can be seen that the reconstruction result by shift estimation (SE) method is almost identical to the true values. The measurement accuracy is significantly improved and the reconstructed surface is much smoother than using PSP method.

Fig.3 shows the absolute errors of reconstructed height distribution. The solid line and dashed line represent the reconstruction error by using PSP method and shift estimation (SE) method respectively. In our simulation, the average absolute

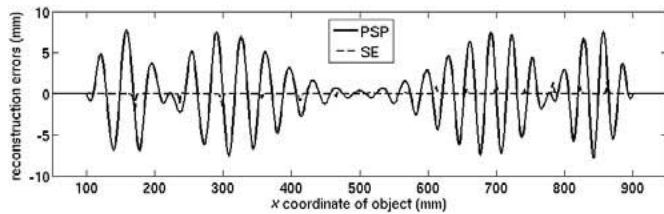


Fig. 3. Absolute reconstruction errors

error and the standard error of the height distribution reconstructed by PSP are 2.7270mm and 3.5268mm. Comparatively by shift estimation (SE) method, the average absolute error and the standard error can be reduced to be only 0.0643mm and 0.2055mm respectively. We can see that measurement accuracy is significantly improved by the generalized model and shift estimation (SE) method.

V. CONCLUSION

In this paper, we have presented a generalized model for fringe pattern profilometry (FPP), which describes a general relationship between the projected signal and the deformed signal. Based on the generalized model, we present a new method, called shift estimation (SE) method for profilometry. With the generalized model and shift estimation (SE) method, the constraint of using sinusoidal signals has been completely removed. In other words, even if the original signal is distorted by some unknown factors, we can still obtain an accurate reconstruction result without any prior knowledge of the characteristics of the profilometry system. The correctness of the generalized model and effectiveness of shift estimation (SE) method have been confirmed by our simulation results.

REFERENCES

- [1] R. Green, J. Walker, and D. Robinson, "Investigation of the fourier-transform method of fringe pattern analysis," *Optics and Lasers in Engineering*, vol. 8, pp. 29–44, 1988.
- [2] X. Su and W. Chen, "Fourier transform profilometry: a review," *Optics and Lasers in Engineering*, vol. 35, pp. 263–284, 2001.
- [3] J. Yi and S. Huang, "Modified fourier transform profilometry for the measurement of 3-d steep shapes," *Optics and Lasers in Engineering*, vol. 27, pp. 493–505, 1997.
- [4] X. Su, W. Chen, Q. Zhang, and Y. Chao, "Dynamic 3-d shape measurement method based on ftp," *Optics and Lasers in Engineering*, vol. 36, pp. 49–64, 2001.
- [5] J. Pearson, F. Lilley, D. Burton, J. Atkinson, S. Kshirsagar, D. Search, and C. Hobson, "Phase-measuring methods for the measurement of three-dimensional shape in automated inspection of manufactured electronic assemblies," in *SPIE Proceedings 2183, Machine Vision Applications in Industrial Inspection II*, 1994, pp. 238–248.
- [6] V. Srinivasan, H. Liu, and M. Halioua, "Automated phase-measuring profilometry of 3-d diffuse objects," *Applied Optics*, vol. 23, pp. 3105–3108, 1984.
- [7] X. Su, W. Zhou, von Bally G, and D. Vukicevic, "Automated phase-measuring profilometry using defocused projection of ronchi grating," *Optics Communication*, vol. 94, pp. 561–573, 1992.
- [8] H. Su, J. Li, and X. Su, "Phase algorithm without the influence of carrier frequency," *Optics Engineering*, vol. 36, pp. 1799–1805, 1997.

- [9] S. Toyooka and Y. Iwaasa, "Automatic profilometry of 3-d diffuse objects by spatial phase detection," *Applied Optics*, vol. 25, pp. 1630–1633, 1986.
- [10] R. Rodriguez-Vera and M. Servin, "Phase locked loop profilometry," *Optics and Lasers Technology*, vol. 26, pp. 393–398, 1994.
- [11] A. Moore and F. Mendoza-Santoyo, "Phase demodulation in the space domain without a fringe carrier," *Optics and Lasers in Engineering*, vol. 23, pp. 319–330, 1995.
- [12] J. Villa, M. Servin, and L. Castillo, "Profilometry for the measurement of 3-d object shapes based on regularized filters," *Optics Communication*, vol. 161, pp. 13–18, 1999.
- [13] L. Kinell, "Multichannel method for absolute shape measurement using projected fringes," *Optics and Lasers in Engineering*, vol. 41, pp. 57–71, 2004.
- [14] P. Huang, Q. Ho, F. Jin, and F. Chiang, "Colour-enhanced digital fringe projection technique for high-speed 3d surface contouring," *Opt Eng*, vol. 38, pp. 1065–1071, 1999.
- [15] Y. Hu, J. Xi, E. Li, J. Chicharo, Z. Yang, and Y. Yu, "A calibration approach for decoupling colour cross-talk using nonlinear blind signal separation network," in *IEEE Conference on Optoelectronic and Microelectronic Materials and Devices*, 2004.
- [16] F. Berryman, P. Pynsent, and J. Cubillo, "A theoretical comparison of three fringe analysis method for determining the three dimensional shape of an object in the present of noise," *Optics and Lasers in Engineering*, vol. 39, pp. 35–50, 2003.